Intelligent Vehicle Power Management: An Overview

Yi L. Murphey

Department of Electrical and Computer Engineering, University of Michigan-Dearborn, Dearborn, MI 48128, USA

Summary. This chapter overviews the progress of vehicle power management technologies that shape the modern automobile. Some of these technologies are still in the research stage. Four in-depth case studies provide readers with different perspectives on the vehicle power management problem and the possibilities that intelligent systems research community can contribute towards this important and challenging problem.

1 Introduction

Automotive industry is facing increased challenges of producing affordable vehicles with increased electrical/electronic components in vehicles to satisfy consumers' needs and, at the same time, with improved fuel economy and reduced emission without sacrificing vehicle performance, safety, and reliability. In order to meet these challenges, it is very important to optimize the architecture and various devices and components of the vehicle system, as well as the energy management strategy that is used to efficiently control the energy flow through a vehicle system [15].

Vehicle power management has been an active research area in the past two decades, and more intensified by the emerging hybrid electric vehicle technologies. Most of these approaches were developed based on mathematical models or human expertise, or knowledge derived from simulation data. The application of optimal control theory to power distribution and management has been the most popular approach, which includes linear programming [47], optimal control [5, 6, 10], and especially dynamic programming (DP) have been widely studied and applied to a broad range of vehicle models [2, 16, 22, 29, 41]. In general, these techniques do not offer an on-line solution, because they assume that the future driving cycle is entirely known. However these results have been widely used as a benchmark for the performance of power control strategies. In more recently years, various intelligent systems approaches such as neural networks, fuzzy logic, genetic algorithms, etc., have been applied to vehicle power management [3, 9, 20, 22, 32, 33, 38, 40, 42, 43, 45, 51, 52]. Research has shown that driving style and environment has strong influence over fuel consumption and emissions [12, 13]. In this chapter we give an overview on the intelligent systems approaches applied to optimizing power management at the vehicle level in both conventional and hybrid vehicles. We present four in-depth case studies, a conventional vehicle power controller, three different approaches for a parallel HEV power controller, one is a system of fuzzy rules generated from static efficiency maps of vehicle components, a system of rules generated from optimal operation points from a fixed driving cycles with using Dynamic Programming and neural networks, and a fuzzy power controller that incorporates intelligent predictions of driving environment as well as driving patterns. We will also introduce the intelligent system research that can be applied to predicting driving environment and driving patterns, which have strong influence in vehicle emission and fuel consumption.

Y.L. Murphey: *Intelligent Vehicle Power Management: An Overview*, Studies in Computational Intelligence (SCI) **132**, 169–190 (2008)
www.springerlink.com

2 Intelligent Power Management in a Conventional Vehicle System

Most road side vehicles today are standard conventional vehicles. Conventional vehicle systems have been going through a steady increase of power consumption over the past twenty years (about 4% per year) [23, 24, 35]. As we look ahead, automobiles are steadily going through electrification changes: the core mechanical components such as engine valves, chassis suspension systems, steering columns, brake controls, and shifter controls are replaced by electromechanical, mechatronics, and associated safety critical communications and software technologies. These changes place increased (electrical) power demands on the automobile [15].

To keep up with future power demands, automotive industry has increased its research in building more powerful power net such as a new 42-V power net topologies which should extend (or replace) the traditional 14-V power net from present vehicles [11, 21], and energy efficiency components, and vehicle level power management strategies that minimize power loss [40]. In this section, we introduce an intelligent power management approach that is built upon an energy management strategy proposed by Koot, et al. [22]. Inspired by the research in HEVs, Koot et al. proposed to use an advanced alternator controlled by power and directly coupled to the engine's crankshaft. So by controlling the output power of alternator, the operating point of the combustion engine can be controlled, thus the control of the fuel use of the vehicle.

Figure 1 is a schematic drawing of power flow in a conventional vehicle system. The drive train block contains the components such as clutch, gears, wheels, and inertia. The alternator is connected to the engine with a fixed gear ratio. The power flow in the vehicle starts with fuel that goes into the internal combustion engine. The mapping from fuel consumed to P_{eng} is a nonlinear function of P_{eng} and engine crank speed ω, denoted as fuel rate = $F(P_{eng}, \omega)$, which is often represented through an engine efficiency map (Fig. 2a) that describes the relation between fuel consumption, engine speed, and engine power.

The mechanical power that comes out of the engine, P_{eng}, splits up into two components: i.e. $P_{eng} = P_p + P_g$, where P_p goes to the mechanical drive train for vehicle propulsion, whereas P_g goes to the alternator. The alternator converts mechanical power P_g to electric power P_e and tries to maintain a fixed voltage level on the power net. The alternator can be modeled as a nonlinear function of the electric power and engine crank speed, i.e. $P_g = G(P_e, \omega)$, which is a static nonlinear map (see Fig. 2b). The alternator provides electric power for the electric loads, P_l, and P_b, power for charging the battery, i.e. $P_e = P_l + P_b$. In the end, the power becomes available for vehicle propulsion and for electric loads connected to the power net. The power flow through the battery, P_b, can be positive (in charge state) or negative (in discharge state), and the power input to the battery, P_b, is more than the actual power stored into the battery, P_s, i.e. there is a power loss during charge and discharge process.

A traditional lead-acid battery is often used in a conventional vehicle system for supplying key-off loads and for making the power net more robust against peak-power demands. Although the battery offers freedom to the alternator in deciding when to generate power, this freedom is generally not yet used in the current practice, which is currently explored by the research community to minimize power loss. Let P_Loss_{bat} represents the power losses function of the battery. P_Loss_{bat} is a function of P_s, E_s and T, where P_s is the

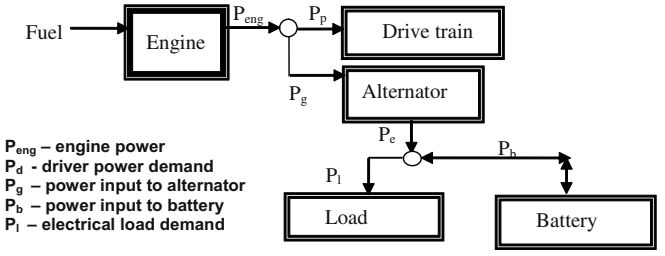

Fig. 1. Power flow in a conventional vehicle system

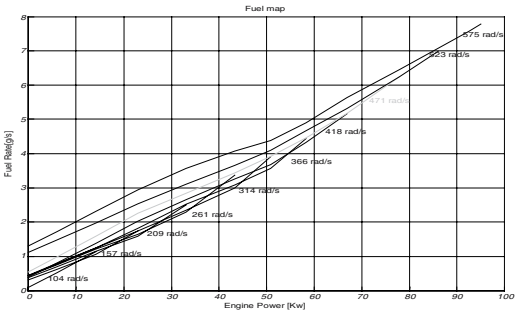

(a) engine efficiency map

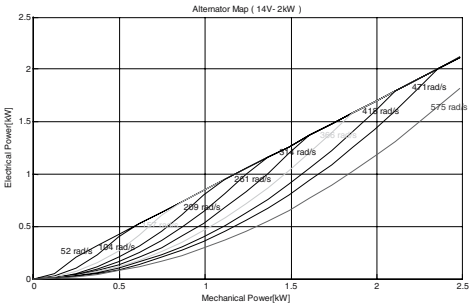

(b) alternator efficiency map

Fig. 2. Static efficiency maps of engine and alternator

power to be stored to or discharged from the battery, E_s is the Energy level of the battery and T is the temperature. To simply the problem, the influence of E_s and T are often ignored in modeling the battery power loss, then P_b can be modeled as a quadratic function of P_s, i.e. $P_b \approx P_s + \beta P_s^2$ [22]. The optimization of power control is driven by the attempt to minimize power loss during the power generation by the internal combustion engine, power conversion by the alternator, and battery charge/discharge.

Based on the above discussion, we are able to model fuel consumption as a function of ω, P_p, P_l, P_s. In order to keep driver requests fulfilled, the engine speed ω, propulsion power P_p, and electric load P_l are set based on driver's command. Therefore the fuel consumption function can be written as a nonlinear function of only one variable $P_s : \gamma(P_s)$.

One approach to intelligent power control is to derive control strategies from the analysis of global optimization solution. To find the global optimal solution, quadratic and dynamic programming (DP) have been extensively studied in vehicle power management. In general, these techniques do not offer an on-line solution, because they assume that the future driving cycle is entirely known. Nevertheless, their results can be used as a benchmark for the performance of other strategies, or to derive rules for a rule-based strategy. In particular if the short-term future state is predictable based on present and past vehicle states of the same driving cycle, the knowledge can be used in combination with the optimization solution to find effective operating points of the individual components.

The cost function for the optimization is the fuel used during an entire driving cycle: $\int_0^{t_e} \gamma(P_s)\mathrm{d}t$ where $[0,\ t_e]$ is the time interval for the driving cycle. When the complete driving cycle is known a priori, the

global optimization of the cost function can be solved using either DP or QP with constraints imposed on P_s. But, for an online controller, it has no knowledge about the future of the present driving cycle. Koot et al. proposed an online solution by using Model Predict Control strategy based on QP optimization [22].

The cost function $\gamma(P_s)$ can be approximated by a convex quadratic function:

$$\gamma(P_s) \approx \varphi_2 \cdot P_s^2 + \varphi_1 \cdot P_s + \varphi_0, \quad \varphi_2 > 0. \tag{1}$$

The optimization problem thus can be model as a multistep decision problem with N steps:

$$\underset{\bar{P}_s}{\text{Min}}\, J = \sum_{k=1}^{N} \min_{P_s} \gamma(P_s(k), k) \approx \sum_{k=1}^{N} \min_{P_s} \frac{1}{2}\varphi_2 P_s^2(k) + \varphi_1(k) P_s(k) + \varphi_0, \tag{2}$$

where $\bar{P}_s$ contains the optimal setting of $P_s(k)$, for $k = 0, \ldots, n$, n is the number of time intervals in a given driving cycle has. The quadratic function of the fuel rate is solved by minimizing the following Lagrange function of with respect to P_s and λ:

$$L(Ps(1), \ldots, Ps(N), \lambda) = \sum_{k=1}^{N} \{\varphi_2(k) Ps(k)^2 + \varphi_1(k) Ps(k)\} + \varphi_0 - \lambda \sum_{k=1}^{N} Ps(k). \tag{3}$$

The optimization problem is solved by taking the partial derivatives of Lagrange function L with respect to $P_s(k)$, $k = 1, \ldots$ to N and λ respectively and setting both equations to 0. This gives us the optimal setting points

$$P_s^o(k) = \frac{\lambda - \varphi_1(k)}{2\varphi_2(k)}, \tag{4}$$

$$\lambda = \sum_{k=1}^{N} \frac{\varphi_1(k)}{2\varphi_2(k)} \Big/ \sum_{k=1}^{N} \frac{1}{2\varphi_2(k)}, \tag{5}$$

for $k = 1, \ldots, N$ (driving time span).

The above equations show that $P_s^o(k)$ depends on the Quadratic coefficients at the current time k, which can be obtained online; however, λ requires the knowledge of φ_1 and φ_2 over the entire driving cycle, which is not available to an online controller. To solve this problem, Koot et al. proposed to estimate λ dynamically using the PI-type controller as follows [22]:

$$\lambda(k+1) = \lambda_0 + Kp(Es(0) - Es(k)) + K_I \sum_{i=1}^{k} (Es(0) - Es(i))\Delta t, \tag{6}$$

where λ_0 is an initial estimate. If we write the equation in an adaptive form, we have

$$\begin{aligned} \lambda(k+1) &= \lambda_0 + K_p(E_s(0) - E_s(k-1) + E_s(k-1) - E_s(k)) + K_I \sum_{i=1}^{k} (E_s(0) - E_s(i))\Delta t \\ &= \lambda(k) + K_p(E_s(k-1) - E_s(k)) + K_I(E_s(0) - E_s(k))\Delta t. \end{aligned} \tag{7}$$

By incorporating $E_s(k)$, the current energy storage in the battery, into λ dynamically, we are able to avoid draining or overcharging the battery during the driving cycle. The dynamically changed λ reflects the change of the stored energy during the last step of the driving cycle, and the change of stored energy between current and the beginning of the driving cycle. If the stored energy increased (or decreased) in comparison to its value the last step and the initial state, the $\lambda(k+1)$ will be much smaller (greater) than $\lambda(k)$.

Koot [25] suggested the following method to tune the PI controller in (6). λ_0 should be obtained from the global QP optimization and is electric load dependant. $\lambda_0 = 2.5$ was suggested. K_P and K_I were tuned such that for average values of $\varphi_1(t)$ and $\varphi_2(t)$ (6) becomes a critically damped second-order system. For $\bar{\varphi}_2 = 1.67 \times 10^{-4}$, $K_p = 6.7 \times 10^{-7}$, $K_I = 3.3 \times 10^{-10}$.

Based on the above discussion, the online control strategy proposed by Koot can be summarized as follows. During an online driving cycle at step k, the controller performs the following three major computations:

(1) Adapt the Lagrange multiplier,

$$\lambda(k+1) = \lambda_0 + K_p(E_s(0) - E_s(k-1) + E_s(k-1) - E_s(k)) + K_1 \sum_{i=1}^{k} (E_s(0) - E_s(i))\Delta t,$$

where λ_0, K_p, K_I are tuned to constants as we discussed above, E_s (i) is the energy level contained in the battery at step i, i = 0, 1, . . . , k, and for i = 0, it is the battery energy level at the beginning of the driving cycle. All E_s (i) are available from the battery sensor.

(2) Calculate the optimal P_s(k) using the following either one of the two formulas:

$$P_s^o(k) = \arg\min_{P_s(k)} \{\varphi_2(k)P_s^2(k) + \varphi_1(k)P_s(k) + \varphi_0(k) - \lambda(k+1)P_s(k), \tag{8}$$

or

$$P_s^o(k) = \arg\min_{P_s(k)} \{\gamma(P_s(k)) - \lambda(k+1)P_s(k)\}. \tag{9}$$

Both methods search for the optimal P_s(k) within its valid range at step k [22], which can be solved using DP with a horizon length of 1 on a dense grid. This step can be interpreted as follows. At each time instant the actual incremental cost for storing energy is compared with the average incremental cost. Energy is stored when generating now is more beneficial than average, whereas it is retrieved when it is less beneficial.

(3) Calculate the optimal set point of engine power
The optimal set point of engine power can be obtained through the following steps:

$$P_{eng}^o = P_g^o + P_p, \text{ where } P_g^o = \mathrm{G}(P_e^o, \omega), P_e^o = \mathrm{P\_Loss_{bat}}(P_s^o) + \mathrm{P_1}.$$

Koot et al. implemented their online controllers in a simulation environment in which a conventional vehicle model with the following components was used: a 100-kW 2.0-L SI engine, a manual transmission with five gears, A 42-V 5-kW alternator and a 36-V 30-Ah lead-acid battery make up the alternator and storage components of the 42-V power net. Their simulations show that a fuel reduction of 2% can be obtained by their controllers, while at the same time reducing the emissions. The more promising aspect is that the controller presented above can be extended to a more intelligent power control scheme derived from the knowledge about road type and traffic congestions and driving patterns, which are to be discussed in Sect. 4.

3 Intelligent Power Management in Hybrid Vehicle Systems

Growing environmental concerns coupled with the complex issue of global crude oil supplies drive automobile industry towards the development of fuel-efficient vehicles. Advanced diesel engines, fuel cells, and hybrid powertrains have been actively studied as potential technologies for future ground vehicles because of their potential to significantly improve fuel economy and reduce emissions of ground vehicles. Due to the multiple-power-source nature and the complex configuration and operation modes, the control strategy of a hybrid vehicle is more complicated than that of a conventional vehicle. The power management involves the design of the high-level control algorithm that determines the proper power split between the motor and the engine to minimize fuel consumption and emissions, while satisfying constraints such as drivability, sustaining and component reliability [28]. It is well recognized that the energy management strategy of a hybrid vehicle has high influences over vehicle performances.

In this section we focus on the hybrid vehicle systems that use a combination of an internal combustion engine (ICE) and electric motor (EM). There are three different types of such hybrid systems:

- Series Hybrid: In this configuration, an ICE-generator combination is used for providing electrical power to the EM and the battery.

- Parallel Hybrid: The ICE in this scheme is mechanically connected to the wheels, and can therefore directly supply mechanical power to the wheels. The EM is added to the drivetrain in parallel to the ICE, so that it can supplement the ICE torque.
- Series–Parallel Combined System and others such as Toyota Hybrid System (THS).

Most of power management research in HEV has been in the category of parallel HEVs. Therefore this is also the focus of this paper. The design of a HEV power controller involves two major principles:

- Meet the driver's power demand while achieving satisfactory fuel consumption and emissions.
- Maintain the battery state of charge (SOC) at a satisfactory level to enable effective delivery of power to the vehicle over a wide range of driving situations.

Intelligent systems technologies have been actively explored in power management in HEVs. The most popular methods are to generate rules of conventional or fuzzy logic, based on:

- Heuristic knowledge on the efficient operation region of an engine to use the battery as a load-leveling component [46].
- Knowledge generated by optimization methods about the proper split between the two energy sources determined by minimizing the total equivalent consumption cost [26, 29, 30]. The optimization methods are typically Dynamic Programming (deterministic or stochastic).
- Driving situation dependent vehicle power optimization based on prediction of driving environment using neural networks and fuzzy logic [27, 42, 52].

Three case studies will be presented in the following subsections, one from each of the above three categories.

3.1 A Fuzzy Logic Controller Based on the Analysis of Vehicle Efficiency Maps

Schouten, Salman and Kheir presented a fuzzy controller in [46] that is built based on the driver command, the state of charge of the energy storage, and the motor/generator speed. Fuzzy rules were developed for the fuzzy controller to effectively determine the split between the two powerplants: electric motor and internal combustion engine. The underlying theme of the fuzzy rules is to optimize the operational efficiency of three major components, ICE (Internal Combustion Engine), EM (Electric Motor) and Battery.

The fuzzy control strategy was derived based on five different ways of power flow in a parallel HEV: (1) provide power to the wheels with only the engine; (2) only the EM; or (3) both the engine and the EM simultaneously; (4) charge the battery, using part of the engine power to drive the EM as a generator (the other part of ENGINE power is used to drive the wheels); (5) slow down the vehicle by letting the wheels drive the EM as a generator that provides power to the battery (regenerative braking).

A set of nine fuzzy rules was derived from the analysis of static engine efficiency map and motor efficiency map with input of vehicle current state such as SOC and driver's command. There are three control variables, SOC (battery state of charge), P_{driver} (driver power command), and ω_{EM} (EM speed) and two solution variables, P_{gen} (generator power), scale factor, SF.

The driver inputs from the brake and accelerator pedals were converted to a driver power command. The signals from the pedals are normalized to a value between zero and one (zero: pedal is not pressed, one: pedal fully pressed). The braking pedal signal is then subtracted from the accelerating pedal signal, so that the driver input takes a value between -1 and $+1$. The negative part of the driver input is sent to a separate brake controller that will compute the regenerative braking and the friction braking power required to decelerate the vehicle. The controller will always maximize the regenerative braking power, but it can never exceed 65% of the total braking power required, because regenerative braking can only be used for the front wheels.

The positive part of the driver input is multiplied by the maximum available power at the current vehicle speed. This way all power is available to the driver at all times [46]. The maximum available power is computed by adding the maximum available engine and EM power. The maximum available EM and engine power depends on EM/engine speed and EM/engine temperature, and is computed using a two-dimensional

look-up table with speed and temperature as inputs. However, for a given vehicle speed, the engine speed has one out of five possible values (one for each gear number of the transmission). To obtain the maximum engine power, first the maximum engine power levels for those five speeds are computed, and then the maximum of these values is selected.

Once the driver power command is calculated, the fuzzy logic controller computes the optimal generator power for the EM, P_{gen}, in case it is used for charging the battery and a scaling factor, SF, for the EM in case it is used as a motor. This scaling factor SF is (close to) zero when the SOC of the battery is too low. In that case the EM should not be used to drive the wheels, in order to prevent battery damage. When the SOC is high enough, the scaling factor equals one.

The fuzzy control variable P_{drive} has two fuzzy terms, normal and high. The power range between 0 and 50 kw is for "normal", the one between 30 kw to the maximum is for "high", the power range for the transition between normal and high, i.e. 30 kw $\sim$ 50 kW, is the optimal range for the engine. The fuzzy control variable SOC has four fuzzy terms, too low, low, normal and too high. The fuzzy set for "too low" ranges from 0 to 0.6, "low" from 0.5 to 0.75, "normal" from 0.7 to 0.9, "too high" from 0.85 to 1.

The fuzzy control variable ω_{EM} (EM speed) has three fuzzy sets, "low", "optimal", and "high". The fuzzy set "low" ranges from 0 to 320 rad s^{-1}, "optimal" ranges from 300 to 470 rad s^{-1}, "high" from 430 through 1,000 rad s^{-1}. Fuzzy set "optimal" represents the optimal speed range which gives membership function to 1 at the range of 320 rad s^{-1} through 430 rad s^{-1}. The nine fuzzy rules are shown in Table 1.

Rule 1 states that if the SOC is too high the desired generator power will be zero, to prevent overcharging the battery. If the SOC is normal (rules 2 and 3), the battery will only be charged when both the EM speed is optimal and the driver power is normal. If the SOC drops to low, the battery will be charged at a higher power level. This will result in a relatively fast return of the SOC to normal. If the SOC drops to too low (rules 6 and 7), the SOC has to be increased as fast as possible to prevent battery damage. To achieve this, the desired generator power is the maximum available generator power and the scaling factor is decreased from one to zero. Rule 8 prevents battery charging when the driver power demand is high and the SOC is not too low. Charging in this situation will shift the engine power level outside the optimum range (30–50 kW). Finally, when the SOC is not too low (rule 9), the scaling factor is one.

The engine power, P_{eng}, and EM power, P_{EM}, are calculated as follows:

$$P_{eng} = P_{driver} + P_{gen}, P_{EM} = -P_{gen}$$

except for the following cases:

(1) If $P_{driver} + P_{EM,gen}$ is smaller than the threshold value SF*6 kw) then $P_{eng} = 0$ and $P_{EM} = P_{driver}$.
(2) If $P_{driver} + P_{EM,gen}$ is larger than the maximum engine power at current speed ($P_{eng,max@speed}$) then

$$P_{eng} = P_{eng,max@speed} \text{and } P_{EM} = P_{driver} - P_{eng,max@speed}.$$

(3) If P_{EM} is positive (EM used as motor), $P_{EM} = P_{EM}$*SF.

The desired engine power level is used by the gear shifting controller to compute the optimum gear number of the automated manual transmission. First, the optimal speed-torque curve is used to compute

Table 1. Rule base of the fuzzy logic controller

1	If SOC is too high then P_{gen} is 0 kw
2	If SOC is normal and P_{drive} is normal and ω_{EM} is optimal then P_{gen} is 10 kw
3	If SOC is normal and ω_{EM} is NOT optimal then P_{gen} is 0 kw
4	If SOC is low and P_{drive} is normal and ω_{EM} is low then P_{gen} is 5 kw
5	If SOC is low and P_{drive} is normal and ω_{EM} is NOT low then P_{gen} is 15 kw
6	If SOC is too low then P_{gen} is $P_{gen,\ max}$
7	If SOC is too low then SF is 0
8	If SOC is NOT too low and P_{drive} is high then P_{gen} is 0 kw
9	If SOC is NOT too low then SF is 1

the optimal engine speed and torque for the desired engine power level. The optimal engine speed is then divided by the vehicle speed to obtain the desired gear ratio. Finally, the gear number closest to the desired gear ratio is chosen.

The power controller has been implemented and simulated with PSAT using the driving cycles described in the SAE J1711 standard. The operating points of the engine, EM, and battery were either close to the optimal curve or in the optimal range [46].

3.2 An Intelligent Controller Built Using DP Optimization and Neural Networks

Traditional rule-based algorithms such as the one discussed in Sect. 3.1 are popular because they are easy to understand. However, when the control system is multi-variable and/or multi-objective, as often the case in HEV control, it is usually difficult to come up with rules that capture all the important trade-offs among multiple performance variables. Optimization algorithms such as Dynamic Programming (DP) can help us understand the deficiency of the rules, and subsequently serve as a "role-model" to construct improved and more complicated rules [28, 41]. As Lin et al. pointed out that using a rule-base algorithm which mimics the optimal actions from the DP approach gives us three distinctive benefits: (1) optimal performance is known from the DP solutions; (2) the rule-based algorithm is tuned to obtain near-optimal solution, under the pre-determined rule structure and number of free parameters; and (3) the design procedure is re-useable, for other hybrid vehicles, or other performance objectives [28].

Lin et al. designed a power controller for a parallel HEV that uses deterministic dynamic programming (DP) to find the optimal solution and then extracts implementable rules to form the control strategy [28, 29]. Figure 3 gives the overview of the control strategy. The rules are extracted from the optimization results generated by two runs of DP, one is running with regeneration on, and the other with regeneration off. Both require the input of a HEV model and a driving cycle. The DP running with regeneration on generates results from which rules for gear shift logic and power split strategy are extracted, the DP running with regeneration off generates results for rules for charge-sustaining strategy.

When used online, the rule-based controller starts by interpreting the driver pedal motion as a power demand, P_d. When P_d is negative (brake pedal pressed), the motor is used as a generator to recover vehicle

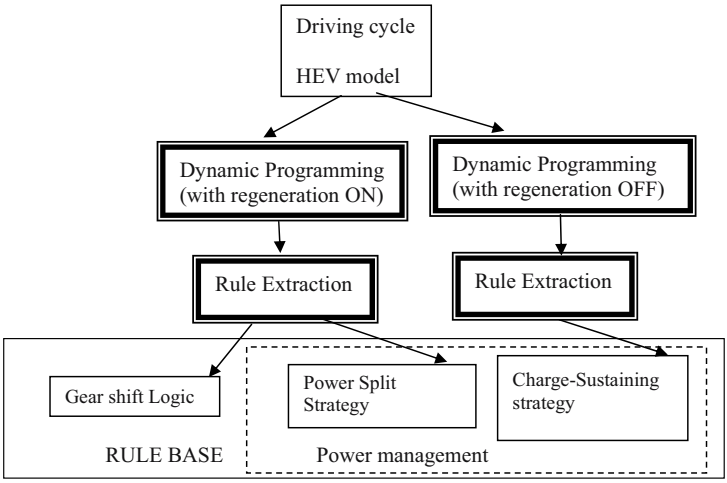

Fig. 3. A rule based system developed based on DP optimization

kinetic energy. If the vehicle needs to decelerate harder than possible with the "electric brake", the friction brake will be used. When positive power ($P_d > 0$) is requested (gas pedal pressed), either a Power Split Strategy or a Charge-Sustaining Strategy will be applied, depending on the battery state of charge (SOC). Under normal driving conditions, the Power Split Strategy determines the power flow in the hybrid powertrain. When the SOC drops below the lower limit, the controller will switch to the Charge-Sustaining Strategy until the SOC reaches a pre-determined upper limit, and then the Power Split Strategy will resume.

The DP optimization problem is formulated as follows. Let x(k) represents three state variables, vehicle speed, SOC and gear number, at time step k, and u(k) are the input signals such as engine fuel rate, transmission shift to the vehicle at time step k. The cost function for fuel consumption is defined as

$$J = fuel = \sum_{k=1}^{N} L(x(k), u(k)), (\text{kg}),$$

where L is the instantaneous fuel consumption rate, and N is the time length of the driving cycle. Since the problem formulated above does not impose any penalty on battery energy, the optimization algorithm tends to first deplete the battery in order to achieve minimal fuel consumption. This charge depletion behavior will continue until a lower battery SOC is reached. Hence, a final state constraint on SOC needs to be imposed to maintain the energy of the battery and to achieve a fair comparison of fuel economy. A soft terminal constraint on SOC (quadratic penalty function) is added to the cost function as follows:

$$J = \sum_{k=1}^{N} L(x(k), u(k)) + G(x(N)),$$

where $G(x(N)) = \alpha(SOC(N) - SOC_f)^2$ represents the penalty associated with the error in the terminal SOC; SOC_f is the desired SOC at the final time, α is a weighting factor. For a given driving cycle, D_C, DP produces an optimal, time-varying, state-feedback control policy that is stored in a table for each of the quantized states and time stages, i.e. $u^*(x(k), k)$; this function is then used as a state feedback controller in the simulations. In addition, DP creates a family of optimal paths for all possible initial conditions. In our case, once the initial SOC is given, the DP algorithm will find an optimal way to bring the final SOC back to the terminal value (SOC_f) while achieving the minimal fuel consumption.

Note that the DP algorithm uses future information throughout the whole driving cycle, D_C, to determine the optimal strategy, it is only optimal for that particular driving cycle, and cannot be implemented as a control law for general, unknown driving conditions. However, it provides good benchmark to learn from, as long as relevant and simple features can be extracted. Lin et al. proposed the following implementable rule-based control strategy incorporating the knowledge extracted from DP results [28]. The driving cycle used by both DP programs is EPA Urban Dynamometer Driving Schedule for Heavy-Duty Vehicles (UDDSHDV) from the ADVISOR drive-cycle library. The HEV model is a medium-duty hybrid electric truck, a 4×2 Class VI truck constructed using the hybrid electric vehicle simulation tool (HE-VESIM) developed at the Automotive Research Center of the University of Michigan [28]. It is a parallel HEV with a permanent magnet DC brushless motor positioned after the transmission. The engine is connected to the torque converter (TC), the output shaft of which is then coupled to the transmission (Trns). The electric motor is linked to the propeller shaft (PS), differential (D) and two driveshafts (DS). The motor can be run reversely as a generator, by drawing power from regenerative braking or from the engine. The detail of this HEV model can be found in [28, 29].

The DP program that ran with regeneration turned on produced power split graph shown in Fig. 4. The graph shows the four possible operating modes in the Power Split Strategy: motor only mode (blue circles), engine only mode (red disks), hybrid mode (both the engine and motor provide power, shown in blue squares), and recharge mode (the engine provides additional power to charge the battery, shown in green diamonds). Note during this driving cycle, recharging rarely happened. The rare occurrence of recharging events implies that, under the current vehicle configuration and driving cycle, it is not efficient to use engine power to charge the battery, even when increasing the engine's power would move its operation to a more efficient region. As a result, we assume there is no recharging during the power split control, other than

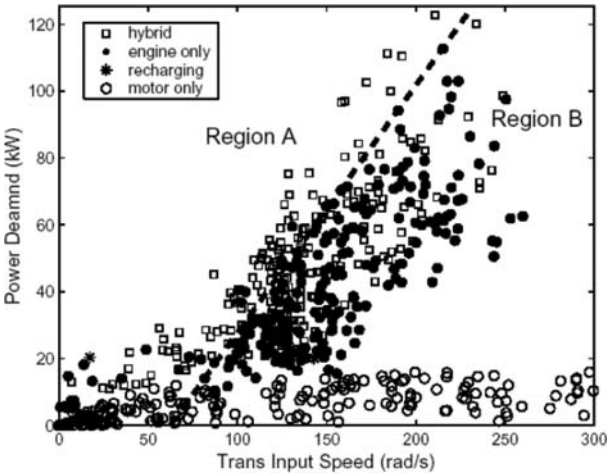

Fig. 4. Optimal operating points generated by DP over UDDSHDV cycle when $P_d > 0$

regeneration, and thus recharge by the engine will only occur when SOC is too low. The following power split rules were generated based on the analysis of the DP results.

$Nnet_1$ is a neural network trained to predict the optimal motor power in a split mode. Since optimal motor power may depend on many variables such as wheel speed, engine speed, power demand, SOC, gear ratio, etc., [28], Lin et al. first used a regression-based program to select the most dominant variables in determining the motor power. Three variables were selected, power demand, engine speed, and transmission input speed as input to the neural network. The neural network has two hidden layers with three and one neurons respectively. After the training, the prediction results generated by the neural network are stored in a "look-up table" for real-time online control.

The efficiency operation of the internal combustion engine also depends on transmission shift logic. Lin et al. used the DP solution chooses the gear position to improve fuel economy. From the optimization results, the gear operation points are expressed on the engine power demand vs. wheel speed plot shown in Fig. 5. The optimal gear positions are separated into four regions, and the boundary between two adjacent regions seems to represent better gear shifting thresholds. Lin et al. use a hysteresis function to generate the shifting thresholds. They also pointed out that the optimal gear shift map for minimum fuel consumption can also be constructed through static optimization. Given an engine power and wheel speed, the best gear position for minimum fuel consumption can be chosen based on the steady-state engine fuel consumption map. They found that the steady-state gear map nearly coincides with Fig. 5. However for a pre-transmission hybrid configuration, it will be harder to obtain optimal shift map using traditional methods.

Since the Power Split Strategy described above does not check whether the battery SOC is within the desired operating range, an additional rule for charging the battery with the engine was developed by Lin et al. to prevent battery from depletion. A traditional practice is to use a thermostat-like charge sustaining strategy, which turns on the recharging mode only if the battery SOC falls below a threshold and the charge continues until the SOC reaches a predetermined level. Although this is an easy to implement strategy, it is not the most efficient way to recharge the battery. In order to improve the overall fuel efficiency further, the questions "when to recharge" and "at what rate" need to be answered. Lin et al. ran the DP routine with the regenerative braking function was turned off to make sure that all the braking power was supplied by the friction braking and hence there was no "free" energy available from the regenerative braking. They set the initial SOC at 0.52 for the purpose of simulating the situation that SOC is too low and the battery needs to be recharged. Their simulation result is shown in Fig. 6.

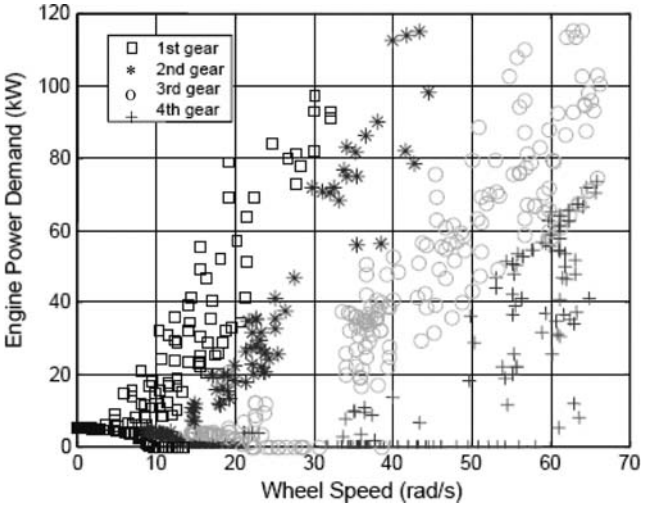

Fig. 5. Transmission gear selection generated by DP algorithm when $P_d > 0$ over UDDSHDV cycle

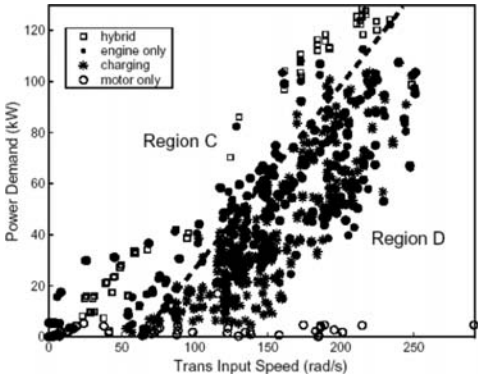

Fig. 6. Optimal operating points from DP (engine recharging scenario) over UDDSHDV cycle

Note that the results obtained represent the optimal policy under the condition that the battery SOC has to be recharged from 0.52 to 0.57 using engine power. Note also that negative motor power now represents the recharging power supplied by the engine since there is no regenerative braking. A threshold line is drawn to divide the plot into two regions C and D. A neural network $Nnet_2$ was trained to find the optimal amount of charging power. The basic logic of this recharging control is summarized in Table 3. The rules in Tables 2 and 3 together provide complete power management of the hybrid propulsion system under any conditions. Figure 7 shows the flow charts of the power controller. T_line1 is the function representing the threshold shown in Fig. 7a, and T_line2 is the function representing the threshold shown in Fig. 7b.

Lin et al. used the Urban Dynamometer Driving Schedule for Heavy-Duty Vehicles (UDDSHDV) to evaluate the fuel economy of their power management strategy. Their results were obtained for the charge

Table 2. Power split rules

If $P_d \leq 15$ kw, use Motor only, i.e. $P_m = P_d,\ P_e = 0$.
Else
If region A, operate in power split mode: $P_m = Nnet_1(P_d, \omega_{trans}, \omega_{eng}), P_e = P_d - P_m$.
If region B, use engine only, i.e. $P_m = 0,\ P_e = P_d$.
If $P_e > P_{e\_max},\ P_e = P_{e\_max},\ P_m = P_d - P_e$.
Note: P_m is the motor power, P_e is the engine power, and P_d is driver's power demand.

Table 3. Charge-sustaining rules

If $P_d \leq 8$ kw, use Motor only, i.e. $P_m = P_d,\ P_e = 0$.
Else
If region C, or $\omega_{wheel} < 10,\ P_e = P_d,\ P_m = 0$.
If region D, $P_m = -P_{ch},\ P_e = P_d + P_{ch},\ P_{ch} = -Nnet_2(P_d, \omega_{trans}, \omega_{eng})$,
If $P_e > P_{e\_max},\ P_e = P_{e\_max},\ P_m = P_d - P_e$.

sustaining strategy, with the SOC at the end of the cycle being the same as it was at the beginning. They showed 28% of the fuel economy improvement (over the conventional truck) by the DP algorithm and 24% by their DP-trained rule-based algorithm, which is quite close to the optimal results generated by the DP algorithm.

3.3 Intelligent Vehicle Power Management Incorporating Knowledge About Driving Situations

The power management strategies introduced in the previous sections do not incorporate the driving situation and/or the driving style of the driver into their power management strategies. One step further is to incorporate the optimization into a control strategy that has the capability of predicting upcoming events. In this section we take introduce an intelligent controller, IEMA (intelligent energy management agent) proposed by Langari and Won [27, 52]. IEMA incorporates true drive cycle analysis within an overall framework for energy management in HEVs. Figure 8 shows the two major components in the architecture of IEMA, where T_e is the current engine torque, $T_{ec,\ FTD}$ is the increment of engine torque for propulsion produced by FTD, and $T_{ec,\ TD}$ is the increment engine torque compensating for the effect of variations of driver style. The primary function of IEMA is to distribute the required torque between the electric motor and the IC (internal combustion) engine. In order to accomplish this, IEMA utilizes information on roadway type and traffic congestion level, driver style, etc., which are produced by intelligent systems discussed in Sect. 4. The FTD is a fuzzy controller that has fuzzy rule sets for each roadway type and traffic congestion level. The SCC, constructed based on expert knowledge about charge sustaining properties in different operating modes, guarantees that the level of electric energy available through the electric energy storage is maintained within a prescribed range throughout the entire driving. Its output, $T_{ec,\ SOC}$, is the increment of engine torque for charging. T_{ec} is engine torque command. The relationship among these variables is characterized as follows:

$$T_{ec} + T_{mc} = T_e + T_{ec,FTD} + T_{ec,SOC} + T_{mc} = T_c, \tag{10}$$

where T_{mc} is motor torque command and T_c is the driver's torque command.

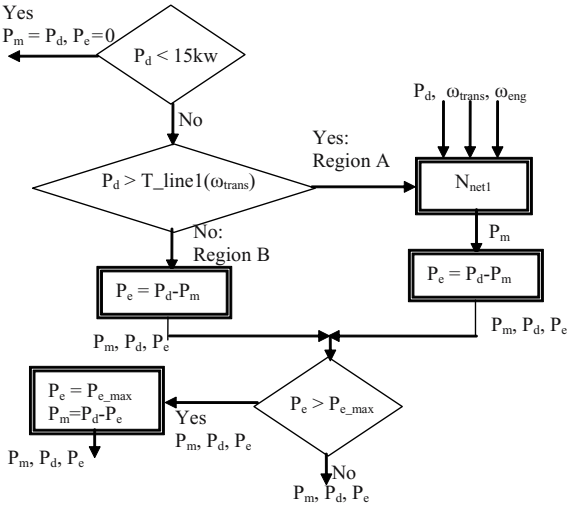

(a) Power split strategy

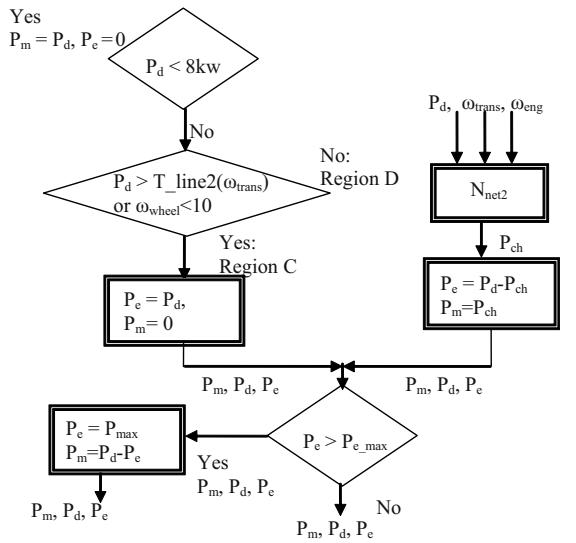

(b) Charge - sustaining strategy

Fig. 7. Power management of the hybrid propulsion system

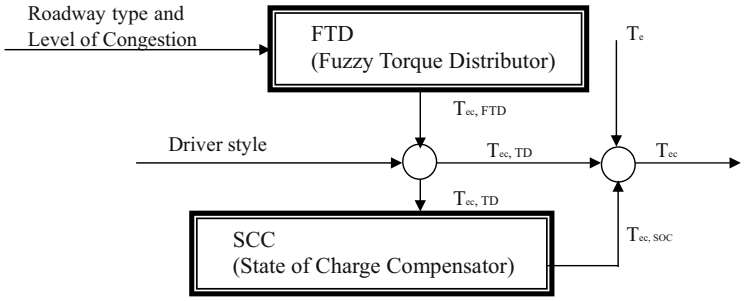

Fig. 8. Architecture view of IEMA proposed by Langari and Won

The function of FTD is to determine the effective distribution of torque between the motor and the engine. FTD is a fuzzy rule based system that incorporates the knowledge about the driving situation into energy optimization strategies. Fuzzy rules are generated for each of the nine facility driving cycles defined by Sierra Research [44]. These knowledge bases are indexed as RT1 through RT9.

Six fuzzy membership functions are generated for assessing driving trends, driving modes and the SOC, and for the output variable of FTD, $T_{ec,\ FTD}$. These fuzzy membership functions are generated by the expert knowledge about the systems' characteristics and the responses of the powertrain components. Fuzzy rules are generated based on the postulate that fuel economy can be achieved by operating the ICE at the efficient region of the engine and by avoiding transient operations that would occur in typical driving situations such as abrupt acceleration or deceleration, frequent stop-and-go. The rational for each fuzzy rule set is given below:

(1) Low-speed cruise trend. This speed range is defined as below 36.66 ft s^{-1} (25 mph) with small acceleration/deceleration rates (within ± 0.5 ft s^{-2}). When the level of the SOC is high, the electric mother (EM) is used to provide the propulsive power to meet the driver's torque demand (T_{dc}). When the SOC is low, ICE is used to generate propulsive power even if it means (temporary) high fuel consumption, since priority is given to maintaining the SOC at certain levels. For low speed region of ICE under low SOC, no additional engine operation for propulsion is made to avoid the ICE operation at inefficient regions of the region. For high engine speed under low SOC, ICE together with EM are used to generate propulsive power. This strategy is applied to all facility-specific drive cycles whenever this driving trend is present.
(2) High-speed cruise trend. This speed range is defined as over 58.65 ft s^{-1} (40 mph) with small acceleration/deceleration rates (within ± 0.5 ft s^{-2}). In this speed range, ICE is sued to provide propulsive power. For speeds over about 55 mph, fuel consumption rate increases with the increase of vehicle speed. Therefore, EM is used in this region to easy the overall fuel usage. Note, the continued use of EM will result in making SCC to act to recover the SOC of the battery. This rule is applied to all facility-specific drive cycles whenever this driving trend is present. Depending on the gear ratio during driving, the engine speed is determined according to the speed of the vehicle. Given the speed of the vehicle, the engine speed will be high or low depending on the gear ratio. For the high-speed region of the engine, ICE is to be operated for generating power according to the level of the SOC. The EM is used for low speed region of the engine.
(3) Acceleration/deceleration trend. In this acceleration/deceleration, fuzzy rules are devised based on the characteristic features of each drive cycle (i.e. each of the nine facility-specific drive cycles), and is derived by comparing with the characteristics of the neighboring drive cycles. The fuzzy rules were derived based on the speed-fuel consumption analysis, and observations of speed profiles for all nine Sierra driving cycles.

The IEMA also incorporates the prediction of driver style into the torque compensation. Langari and Won characterizes the driving style of the driver by using a driving style factor α_{DSI}, which is used to compensate the output of the FTD through the following formula:

$$T_{ec,TD} = T_{ec,FTD}{}^{*}\,(1 + \mathrm{sgn}(T_{ec,FTD})^{*}\alpha_{DSI})\,, \tag{11}$$

where $T_{ec,\ TD}$ is the increment of engine torque compensating for the effect of driver variability, which is represented by α_{DSI}. Combining with (10) with (11) we have

$$T_{ec} + T_{mc} = T_{e} + T_{ec,FTD}{}^{*}\,(1 + \mathrm{sgn}(T_{ec,FTD})^{*}\alpha_{DSI}) + T_{ec,SOC} + T_{mc} = T_{c}. \tag{12}$$

This compensation was devised based on the following assumption. The transient operation of the engine yields higher fuel consumption than steady operation does. Therefore the driver's behavior is predicted and its effect on the engine operation is adjusted. For example, for the aggressive driver, the less use of ICE is implemented to avoid fuel consumption that is due to the transient operation of the engine by the driver. In [52], a maximum 10% of the increment of engine torque was considered for calm drivers, normal 0% and aggressive −10%.

In order to keep the level of electric energy within a prescribed range throughout driving, SCC, the State-of-Charge Compensator was used in IEMA. The SCC detects the current SOC and compares it with the target SOC, and commands additional engine torque command, $T_{ec,\ SOC}$. As shown in (12), the increment of engine torque from SCC is added to (or subtracted from) the current engine torque for the charge (or discharge) operation.

The charge (or discharge) operations are determined by the instantaneous operating mode, which is characterized into start-up, acceleration, cruise, deceleration (braking), and stationary.

Under the charge sustenance concept, the function of the electric motor can be switched to that of a generator to charge the battery for the next use if surplus power from the engine is available. In certain driving modes, however, particularly in acceleration and cruise modes, battery charge by operating ICE is generally not recommended because this may cause the overall performance to deteriorate and/or the battery to be overcharged. Selective battery charge operation may be required, however, for the operation of HEVs in these modes. In the stop (idle) mode, the charge sustaining operation can be accomplished in an efficient region of the engine while maximizing fuel efficiency if applicable or required. While not considered in this study, external charge operation can be accomplished in the stationary (parking) mode of the vehicle. Langari and Won derived functions for $T_{ec,SOC}$ for both hybrid (acceleration, cruise, and deceleration) and stop modes.

In the hybrid mode $T_{ec,\ SOC}$ is determined based on the analysis of the engine-motor torque plane, driver's torque demand, the (engine) torque margin for the charge operation (TMC) and the discharge operation (TMD). The increments of engine torque were obtained by introducing an appropriate function that relates to the current SOC, TMC, and TMD.

The $T_{ec,\ SOC}$ is further adjusted based on the vehicle's mode of operation. The adjustment was implemented by a fuzzy variable β_{hybrid} and then the incremental of engine torque for the charge operation becomes

$$T_{ec,SOC,hybrid} = \beta_{\mathrm{hybrid}} \times T_{ec,SOC},$$

where β_{hybrid} is the output of a mode-based fuzzy inference system that generates a weighted value of [0, 1] to represent the degree of charge according to the vehicle modes. For instance, if the vehicle experiences high acceleration, additional battery charge is prohibited to avoid deteriorating the vehicle performance even in low level of the SOC in the battery. The value of β_{hybrid} is set to zero whenever the level of the SOC is high in all modes. In the cruise or the deceleration mode, battery charge operation is performed according to the engine speed under low SOC level. In the acceleration mode, battery charge operation is dependent on the magnitude of power demand under low SOC level.

The charge sustaining operation in the stop mode is accomplished based on the analysis of efficient region of the engine while maximizing fuel economy and the best point (or region) of operation of the engine and the gear ratio of the transmission device.

Langari and Won evaluated their IEMA system through simulation on the facility-specific drive cycles [7] and the EPA UDDS [1]. For the simulation study, a typical parallel drivetrain with a continuous variable transmission was used. The vehicle has a total mass of 1,655 kg which is the sum of the curb weight of 1,467 kg and the battery weight. An internal combustion engine with a displacement of 0.77 L and peak power of 25 kW was chosen. The electric motor is chosen to meet the acceleration performance (0 to 60 mph in less than 15 s.) To satisfy the requirement for acceleration, a motor with a power of 45 kW is selected. The battery capacity is 6 kW h (21.6 MJ) with a weight of 188 kg and is chosen on the basis of estimated values of the lead acid battery type used in a conventional car. Langari and Won gave a detailed performance analysis based on whether any of the intelligent predictions are used: roadway type, driving trend, driving style and operating mode. Their experiments showed their IEMA gave significant improvements when any and all of these four types knowledge were used in the power management system.

4 Intelligent Systems for Predicting Driving Patterns

Driving pattern exhibited in real driving is the product of the instantaneous decisions of the driver to cope with the (physical) driving environment. It plays an important roll in power distribution and needs to be predicted during real time operation. Driving patterns are generally defined in terms of the speed profile of the vehicle between time interval $[t - \Delta w,\ t]$, where t is the current time instance during a driving experience, and $\Delta w > 0$ is the window size that characterizes the length of the speed profile that should be used to explore driving patterns. Various research work have suggested that road type and traffic condition, trend and style, and vehicle operation modes have various degrees of impacts on vehicle fuel consumptions [4, 7, 8, 12, 13, 31, 49]. However most of the existing vehicle power control approaches do not incorporate the knowledge about driving patterns into their vehicle power management strategies. Only recently research community in intelligent vehicle power control has begun to explore the ways to incorporate the knowledge about online driving pattern into control strategies [19, 26, 27, 52].

This section discusses the research issues related to the prediction of roadway type and traffic congestions, the driving style of the driver, current driving mode and driving trend.

4.1 Features Characterizing Driving Patterns

Driving patterns can be observed generally in the speed profile of the vehicle in a particular environment. The statistics used to characterize driving patterns include 16 groups of 62 parameters [13], and parameters in nine out of these 16 groups critically affect fuel usage and emissions [4, 12]. However it may not necessary to use all these features for predicting a specific driving pattern, and on the other hand, additional new features may be explored as well. For example in [27], Langari and Won used only 40 of the 62 parameters and then added seven new parameters, trip time; trip distance; maximum speed; maximum acceleration; maximum deceleration; number of stops; idle time, i.e. percent of time at speed 0 kph. To develop the intelligent systems for each of the four prediction problems addressed in this section, namely roadway type and traffic congestion level, driver style, operation mode, driving trend, the selection of a good set of features is one of the most important steps. It has been shown in pattern recognition that too many features may degrade system performances. Furthermore, more features imply higher hardware cost in onboard implementation and more computational time. Our own research shows that a small subset of the features used by Langari and Won [27] can give just as good or better roadway predictions [32].

The problem of selecting a subset of optimal features from a given set of features is a classic research topic in pattern recognition and a NP problem. Because the feature selection problem is computationally expensive, research has focused on finding a quasi optimal subset of features, where *quasi optimal* implies good classification performance, but not necessarily the best classification performance. Interesting feature selection techniques can be found in [14, 18, 34].

4.2 A Multi-Class Intelligent System for Predicting Roadway Types

In general a driving cycle can be described as a composition of different types of roadways such as local, freeway, arterial/collector, etc., and different levels of traffic congestions. Under a contract with the Environmental Protection Agency (EPA), Sierra Research Inc. [7] has developed a set of 11 standard driving cycles, called facility-specific (FS) cycles, to represent passenger car and light truck operations over a range of facilities and congestion levels in urban areas. The 11 drive cycles can be divided into four categories, freeway, freeway ramp, arterial, and local. More recently they have updated the data to reflect the speed limit changes in certain freeways [44]. The two categories, freeway and arterial are further divided into subcategories based on a qualitative measure called level of service (LOS) that describe operational conditions within a traffic stream based on speed and travel time, freedom to maneuver, traffic interruptions, comfort, and convenience. Six types of LOS are defined with labels, A through F, with LOS A representing the best operating conditions and LOS F the worst. Each level of service represents a range of operating conditions and the driver's perception of those conditions; however safety is not included in the measures that establish service levels [44, 48]. According to the most recent results [44], the freeway category has been divided into six LOS: freeway-LOS A, through freeway-LOS F; the arterial category into three LOS: Arterial LOS A–B, Arterial LOS C–D, and Arterial LOS E–F. The speed profiles of the 11 Sierra new driving cycles are shown in Fig. 9. The statistical features of these 11 drive cycles are listed in Table 4.

One potential use of facility specific driving cycles in vehicle power management is to learn knowledge about optimal fuel consumption and emissions in each of 11 facility specific driving cycles and apply the knowledge to online control. From the discussion presented in Sect. 3 we can see that most vehicle power management strategies are generally based on a fixed drive cycle, and as such do not deal with the variability in the driving situation. A promising approach is to formulate a driving cycle dependent optimization approach that selects the optimal operation points according to the characteristic features of the drive cycle. The driving cycle specific knowledge can be extracted from all 11 Sierra FS driving cycles through machine learning of the optimal operation points. During the online power control, the power controller needs to predict the current road type and LOS at the current time. Based on the prediction result, the knowledge extracted from the Sierra FS cycle that match the predicted result can be used for the online power controller. The key issue is to develop an intelligent system that can predict the current and a short-term future road type and LOS based on the history of the current driving cycle.

An intelligent system can be developed to classify the current driving environment in terms of roadway type combined with traffic congestion level based on the 11 standard Sierra FS cycles. The intelligent system can be a neural network or decision tree or any other classification techniques. Langari and Won used a learning vector quantization (LVQ) network to classify the current roadway type and congestion level [27]. An LVQ network has a two-stage process. At the first stage, a competitive layer is used to identify the *subclasses* of input vectors. In the second stage, a linear layer is used to combine these subclasses into the appropriate target classes.

The prediction or classification of road type and LOS is on a segment-by-segment basis. Each driving cycle in a training data set is divided into segments of Δw seconds. In [27], Langari and Won used a $\Delta w = 150\,\mathrm{s}$, and adjacent segments are overlapped. Features are extracted from each segment for prediction and classification. The features used in [27] consisting of 40 parameters from the 62 parameters defined by Sierra are considered since the information on the engine speed and gear changing behavior are not provided in the drive cycles under their consideration. In addition, seven other characteristic parameters, which they believe can enhance the system performance are: trip time; trip distance; maximum speed; maximum acceleration; maximum deceleration; number of stops; idle time, i.e. percent of time at speed 0 kph.

An intelligent system that is developed for road type prediction will have multiple target classes, e.g. 11 Sierra road type and LOSs. For an intelligent system that has a relative large number of output classes, it is important to select an appropriate method to model the output classes. In general a multi-class pattern classification problem can be modeled in two system architectures, a single system with multiple output classes or a system of multiple classifiers. The pattern classes can be modeled by using either One-Against-One (OAO), One-Against-ALL (OAA) or P-Against-Q, with $P > 1$ and $Q > 1$. A comprehensive discussion on this topic can be found in [36, 37].

4.3 Predicting Driving Trend, Operation Mode and Driver Style

Driving trends are referring to the short term or transient effects of the drive cycle such as low speed cruise, high speed cruise, acceleration/deceleration, and so on. These driving trends can be predicted using features such as the magnitudes of average speed, acceleration value, starting and ending speed in the past time segment.

The *instantaneous* operating mode of the vehicle at every second is the representation of the driver's intention (desire) for the operation of the vehicle, such as start-up, acceleration, cruise, deceleration (braking), and stationary. For each mode, different energy management strategies are required to control the flow of power in the drivetrain and maintain adequate reserves of energy in the electric energy storage device. The operation mode can be determined by examining the torque relations on the drive shaft. According to [27], the operation modes can be characterized by the two torque features, the torque required for maintaining

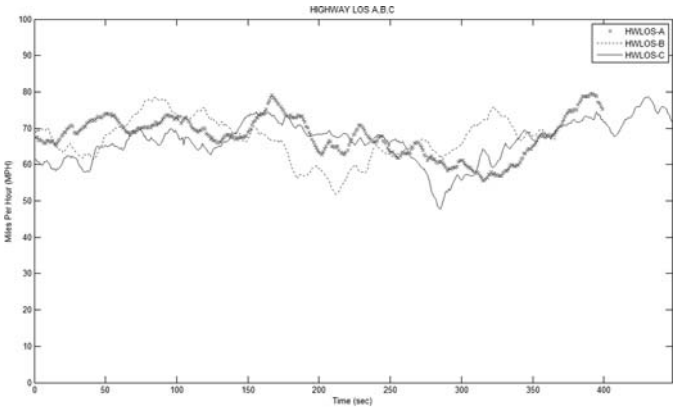

(a) Freeway LOS-A, LOS-B, LOS-C

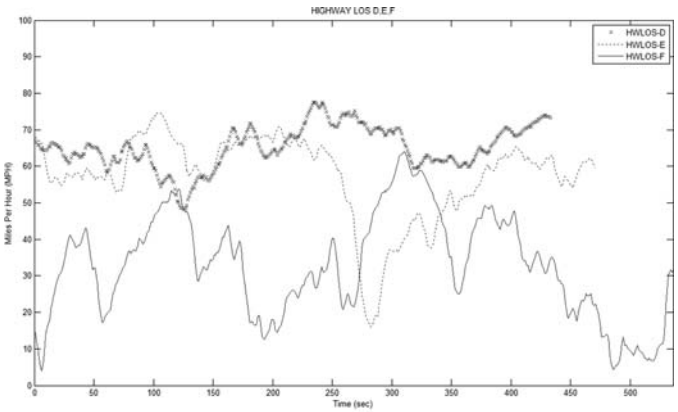

(b) Free Way LOS-D, LOS-E, LOS-F

Fig. 9. New facility specific driving cycles defined by Sierra Research. The speed is in meters per second

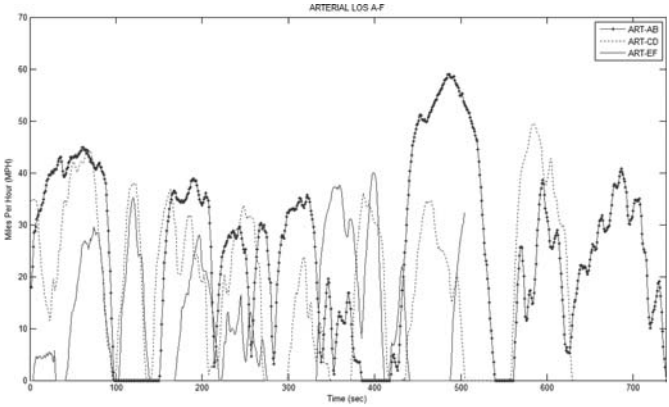

(c) Arterial LOS A-B, LOS C-D, LOS E-F

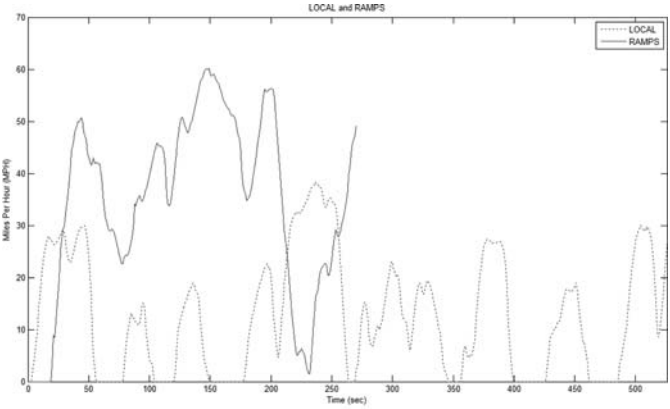

(d) Ramp, Local

Fig. 9. (Continued)

the vehicle speed constant in spite of road load such as rolling resistance, wind drag, and road grade, and the torque required for acceleration or deceleration of the vehicle (driver's command). Langari and Won used the engine speed SP_E is used to infer the road load, which is a function of the road grade and the speed of the vehicle. Under the assumption that mechanical connection between the engine and the wheels through transmission converts the input argument for the speed of the vehicle to the engine speed, and driving occurs on a level road, the road load can be represented by the engine speed.

Driver style or behavior has a strong influence on emissions and fuel consumption [17, 39, 49, 50]. It has been observed that emissions obtained from aggressive driving in urban and rural traffic are much higher than those obtained from normal driving. Similar result is observed in relation to fuel consumption. Drivers style can be categorized in the following three classes [27]:

- *Calm driving* implies anticipating other road user's movement, traffic lights, speed limits, and avoiding hard acceleration.

Table 4. Statistics of 11 facility specific driving cycles

Facility cycles by Sierra Research				
Cycle	V_{avg} (mph)	V_{max} (mph)	A_{max} (mph s^{-2})	Length (s)
Freeway LOS A	67.79	79.52	2.3	399
Freeway LOS B	66.91	78.34	2.9	366
Freeway LOS C	66.54	78.74	3.4	448
Freeway LOS D	65.25	77.56	2.9	433
Freeway LOS E	57.2	74.43	4.0	471
Freeway LOS F	32.63	63.85	4.0	536
Freeway ramps	34.6	60.2	5.7	266
Arterials LOS A–B	24.8	58.9	5.0	737
Arterials LOS C–D	19.2	49.5	5.7	629
Arterials LOS E–F	11.6	39.9	5.8	504
Local roadways	12.9	38.3	3.7	525

- *Normal driving* implies moderate acceleration and braking.
- *Aggressive driving* implies sudden acceleration and heavy braking.

Acceleration criteria for the classification of the driver's style are based on the acceleration ranges can be found in [49]. In [27], a fuzzy classifier was presented. Two fuzzy variables were used, average acceleration and the ratio of the standard deviation (SD) of acceleration and the average acceleration over a specific driving range were used together to identify the driving style.

5 Conclusion

In this chapter we presented an overview of intelligent systems with application to vehicle power management. The technologies used in vehicle power management have evolved from rule based systems generated from static efficiency maps of vehicle components, driving cycle specific optimization of fuel consumption using Quadratic or Dynamic Programming, Predictive control combined with optimization, to the intelligent vehicle power management based on road type prediction and driving patterns such as driving style, operation mode and driving trend. We have seen more and more research in the use of neural networks, fuzzy logic and other intelligent system approaches for vehicle power management.

During the recent years many new telematic systems have been introduced into road vehicles. For instance, global positioning systems (GPS) and mobile phones have become a de facto standard in premium cars. With the introduction of these systems, the amount of information about the traffic environment available in the vehicle has increased. With the availability of traffic information, predictions of the vehicle propulsion load can be made more accurately and efficiently. Intelligent vehicle power systems will have more active roles in building predictive control of the hybrid powertrain to improve the overall efficiency.

References

1. http://www.epa.gov/otaq/emisslab/methods/uddscol.txt
2. I. Arsie, M. Graziosi, C. Pianese, G. Rizzo, and M. Sorrentino, "Optimization of supervisory control strategy for parallel hybrid vehicle with provisional load estimate," in *Proc. 7th Int. Symp. Adv. Vehicle Control (AVEC)*, Arnhem, The Netherlands, Aug. 2004.
3. B. Badreddine and M.L. Kuang, "Fuzzy energy management for powersplit hybrid vehicles," in *Proc. of Global Powertrain Conference*, Sept. 2004.
4. R. Bata, Y. Yacoub, W. Wang, D. Lyons, M. Gambino, and G. Rideout, "Heavy duty testing cycles: survey and comparison," SAE Paper 942 263, 1994.

5. M. Back, M. Simons, F. Kirschaum, and V. Krebs, "Predictive control of drivetrains," in *Proc. IFAC 15th Triennial World Congress*, Barcelona, Spain, 2002.
6. J. Bumby and I. Forster, "Optimization and control of a hybrid electric car," *Inst. Elect. Eng. Proc. D*, vol. 134, no. 6, pp. 373–387, Nov. 1987.
7. T.R. Carlson and R.C. Austin, "Development of speed correction cycles," Report SR97-04-01, Sierra Research, Sacramento, CA, 1997.
8. J. Cloke, G. Harris, S. Latham, A. Quimby, E. Smith, and C. Baughan, "Reducing the environmental impact of driving: a review of training and in-vehicle technologies," Report 384, Transport Res. Lab., Crowthorne, UK, 1999.
9. ZhiHang Chen, M. Abul Masrur, and Yi L. Murphey, "Intelligent vehicle power management using machine learning and fuzzy logic," FUZZ 2008.
10. S. Delprat, J. Lauber, T.M. Guerra, and J. Rimaux, "Control of a parallel hybrid powertrain: optimal control," *IEEE Trans. Veh. Technol.*, vol. 53, no. 3, pp. 872–881, May 2004.
11. A. Emadi, M. Ehsani, and J.M. Miller, *Vehicular Electric Power Systems: Land, Sea, Air, and Space Vehicles*. New York: Marcel Dekker, 2003.
12. E. Ericsson, "Variability in urban driving patterns," *Transport. Res. D*, vol. 5, pp. 337–354, 2000.
13. E. Ericsson, "Independent driving pattern factors and their influence on fuel-use and exhaust emission factors," *Transport. Res. D*, vol. 6, pp. 325–341, 2001.
14. F. Ferri, P. Pudil, M. hatef, and J. Kittler, "Comparative study of techniques for large scale feature selection," in *Pattern Recognition in Practice IV*, E. Gelsema and L. Kanal, eds., pp. 403–413. Amsterdam: Elsevier, 1994.
15. Hamid Gharavi, K. Venkatesh Prasad, and Petros Ioannou, "Scanning advanced automobile technology," *Proc. IEEE*, vol. 95, no. 2, Feb. 2007.
16. T. Hofman and R. van Druten, "Energy analysis of hybrid vehicle powertrains," in *Proc. IEEE Int. Symp. Veh. Power Propulsion*, Paris, France, Oct. 2004.
17. B.A. Holmén and D.A. Niemeier, "Characterizing the effects of driver variability on real-world vehicle emissions," *Transport. Res. D*, vol. 3, pp. 117–128, 1997.
18. Jacob A. Crossman, Hong Guo, Yi Lu Murphey, and John Cardillo, "Automotive Signal Fault Diagnostics: Part I: signal fault analysis, feature extraction, and quasi optimal signal selection," IEEE Transactions on Vehicular Technology, July 2003.
19. S.-I. Jeon, S.-T. Jo, Y.-I. Park, and J.-M. Lee, "Multi-mode driving control of a parallel hybrid electric vehicle using driving pattern recognition," *J. Dyn. Syst. Meas. Control.*, vol. 124, pp. 141–149, Mar. 2002.
20. V.H. Johnson, K.B. Wipke, and D.J. Rausen, "HEV control strategy for real-time optimization of fuel economy and emissions," SAE Paper-01-1543, 2000.
21. K. Ehlers, H.D. Hartmann, and E. Meissner, "42 V – An indication for changing requirements on the vehicle electrical system," *J. Power Sources*, vol. 95, pp. 43–57, 2001.
22. M. Koot, J.T.B.A. Kessels, B. de Jager, W.P.M.H. Heemels, P.P.J. van den Bosch, and M. Steinbuch, "Energy management strategies for vehicular electric power systems," *IEEE Trans. Veh. Technol.*, vol. 54, no. 3, pp. 771–782, May 2005.
23. J.G. Kassakian, J.M. Miller, and N. Traub, "Automotive electronics power up," *IEEE Spectr.*, vol. 37, no. 5, pp. 34–39, May 2000.
24. C. Kim, E. NamGoong, S. Lee, T. Kim, and H. Kim, "Fuel economy optimization for parallel hybrid vehicles with CVT," SAE Paper-01-1148, 1999.
25. M.W.Th. Koot, "Energy management for vehicular electric power systems," Ph.D. thesis, Library Technische Universiteit Eindhoven, 2006, ISBN-10: 90-386-2868-4.
26. I. Kolmanovsky, I. Siverguina, and B. Lygoe, "Optimization of powertrain operating policy for feasibility assessment and calibration: stochastic dynamic programming approach," in *Proc. Amer. Contr. Conf.*, vol. 2, Anchorage, AK, May 2002, pp. 1425–1430.
27. R. Langari and Jong-Seob Won, "Intelligent energy management agent for a parallel hybrid vehicle-part I: system architecture and design of the driving situation identification process," *IEEE Trans. Veh. Technol.*, vol. 54, no. 3, pp. 925–934, 2005.
28. C.-C. Lin, Z. Filipi, L. Louca, H. Peng, D. Assanis and J. Stein, "Modelling and control of a medium-duty hybrid electric truck," *Int. J. Heavy Veh. Syst.*, vol. 11, nos. 3/4, pp. 349–370, 2004.
29. C.-C. Lin, H. Peng, J.W. Grizzle, and J.-M. Kang, "Power management strategy for a parallel hybrid electric truck," *IEEE Trans. Contr. Syst. Technol.*, vol. 11, no. 6, pp. 839–849, Nov. 2003.
30. C.-C. Lin, H. Peng, and J.W. Grizzle, "A stochastic control strategy for hybrid electric vehicles," in *Proc. Amer. Contr. Conf.*, Boston, MI, Jun. 2004, pp. 4710–4715.

31. D.C. LeBlanc, F.M. Saunders, M.D. Meyer, and R. Guensler, "Driving pattern variability and impacts on vehicle carbon monoxide emissions," in *Transport. Res. Rec.*, Transportation Research Board, National Research Council, 1995, pp. 45–52.
32. Yi L. Murphey, ZhiHang Chen, Leo Kiliaris, Jungme Park, Ming Kuang, Abul Masrur, and Anthony Phillips, "Neural learning of predicting driving environment," IJCNN 2008.
33. Jorge Moreno, Micah E. Ortúzar, and Juan W. Dixon, "Energy-management system for a hybrid electric vehicle, using ultracapacitors and neural networks," *IEEE Trans. Ind. Electron.*, vol. 53, no. 2, Apr. 2006.
34. Yi Lu Murphey and Hong Guo, "Automatic feature selection – a hybrid statistical approach," in *International Conference on Pattern Recognition*, Barcelona, Spain, Sept. 3–8, 2000.
35. P. Nicastri and H. Huang, "42 V PowerNet: providing the vehicle electric power for the 21st century," in *Proc. SAE Future Transportation Technol. Conf.*, Costa Mesa, CA, Aug. 2000, SAE Paper 2000-01-3050.
36. Guobing Ou, Yi L. Murphey, and Lee Feldkamp, "Multiclass pattern classification using neural networks," in *International Conference on Pattern Recognition*, Cambridge, UK, 2004.
37. Guobin Ou and Yi Lu Murphey, "Multi-class pattern classification using neural networks," *J. Pattern Recognit.*, vol. 40, no 1, pp. 4–18, Jan. 2007.
38. G. Paganelli, G. Ercole, A. Brahma, Y. Guezennec, and G. Rizzoni, "General supervisory control policy for the energy optimization of charge-sustaining hybrid electric vehicles," *JSAE Rev.*, vol. 22, no. 4, pp. 511–518, Apr. 2001.
39. T. Preben, "Positive side effects of an economical driving style: safety, emissions, noise, costs," in *Proc. ECODRIVE 7th Conf.*, Sept. 16–17, 1999.
40. Danil V. Prokhorov, "Toyota Prius HEV neurocontrol," in *Proceedings of International Joint Conference on Neural Networks*, Orlando, FL, USA, Aug. 12–17, 2007.
41. Danil V. Prokhorov, "Approximating optimal controls with recurrent neural networks for automotive systems," in *Proceedings of the 2006 IEEE International Symposium on Intelligent Control*, Munich, Germany, Oct. 4–6, 2006.
42. Fazal U. Syed, Dimitar Filev, and Hao Ying, "Fuzzy rule-based driver advisory system for fuel economy improvement in a hybrid electric vehicle," in *Annual Meeting of the NAFIPS*, June 24–27, 2007, pp. 178–183.
43. A. Sciarretta, L. Guzzella, and M. Back, "A real-time optimal control strategy for parallel hybrid vehicles with on-board estimation of the control parameters," in *Proc. IFAC Symp. Adv. Automotive Contr.*, Salerno, Italy, Apr. 19–23, 2004.
44. Sierra Research," SCF Improvement – Cycle Development," Sierra Report No. SR2003-06-02, 2003.
45. F. Syed, M.L. Kuang, J. Czubay, M. Smith, and H. Ying, "Fuzzy control to improve high-voltage battery power and engine speed control in a hybrid electric vehicle," in *Soft Computing for Real World Applications, NAFIPS*, Ann Arbor, MI, June 22–25, 2005.
46. N.J. Schouten, M.A. Salman, and N.A. Kheir, "Fuzzy logic control for parallel hybrid vehicles," *IEEE Trans. Contr. Syst. Technol.*, vol. 10, no. 3, pp. 460–468, May 2002.
47. E.D. Tate and S.P. Boyd, "Finding ultimate limits of performance for hybrid electric vehicles," SAE Paper-01-3099, 2000.
48. Highway Capacity Manual 2000, Transportation Res. Board, Washington, DC, 2000.
49. I. De Vlieger, D. De Keukeleere, and J. Kretzschmar, "Environmental effects of driving behaviors and congestion related to passenger cars," *Atmos. Environ.*, vol. 34, pp. 4649–4655, 2000.
50. I. De Vlieger, "Influence of driving behavior on fuel consumption," in *ECODRIVE 7th Conf.*, Sept. 16–17, 1999.
51. J.-S. Won, R. Langari, and M. Ehsani, "Energy management strategy for a parallel hybrid vehicle," in *Proc. Int. Mechan. Eng. Congress and Exposition (IMECE '02)*, New Orleans, LA, Nov. 2002, pp. IMECE2002–33 460.
52. Jong-Seob Won and R. Langari, "Intelligent energy management agent for a parallel hybrid vehicle-part II: torque distribution, charge sustenance strategies, and performance results," *IEEE Trans. Veh. Technol.*, vol. 54, no. 3, pp. 935–953, 2005.